Experimental tests of steel double-type balcony connections

Maciej Tomasz Solarczyk

maciej.solarczyk@pg.edu.pl | ⓘ https://orcid.org/0000-0001-6070-0736

Paweł Piotrkowski

piotrkow@pg.edu.pl | ⓘ https://orcid.org/0000-0001-7860-673X

Maciej Niedostatkiewicz

mniedost@pg.edu.pl | ⓘ https://orcid.org/0000-0002-6451-6220

Gdańsk University of Technology,

Faculty of Civil and Environmental Engineering,

Department of Engineering Structures

Data Availability Statement: All relevant data are within the paper and its Supporting Information files.

Competing interests: The authors have declared that no competing interests exist.

Abstract

This paper presents an analysis and results of experimental tests of full-scale prefabricated balcony sets with dimensions (width × length × height): 2.0 m × 2.78 m × 0.186 m (in a slope to 0.17 m). The sets consist of reinforced concrete slabs (balcony and ceiling) connected with each other with double-type balcony connections. The paper analyses the impact of variable parameters on the load bearing capacity of the elements. Additionally, an overview of current scientific and technical papers in the field of balcony connections is provided.

Keywords: balcony connections, experimental tests, reinforced concrete structures

1. Introduction

The paper analysis the impact of variable parameters on the load-bearing capacity of steel double-type balcony connections (double-type refers to connections consisting of two tension bars and two shear plates connected with each other by a web of C-section), consisting of an undercut C-profile as described in Solarczyk et al. (2019 and 2020), which was a summary of the tests carried out by the authors in Stage I. Solarczyk et al. (2020) also discussed single-type balcony connections consisted of one shear plate welded with one tension bar.

Balcony connection tested in Stage I (Fig. 1) consisted of an undercut C220 profile, 180 mm length connected at the bottom with a transverse plate with a height of 35 mm and a thickness of 12 mm. At the top of the balcony connection, two reinforcement bars $\phi 12$ mm were welded to web of C-profile. The components of the balcony connection (1 and 2 in Fig. 1) were made of S355J2G3 steel. The balcony set was marked as I_ZB_2_1.

In Stage II, the balcony connections presented in Fig. 1 (marked as II_ZB_2_2 and II_ZB_2_3) and in Fig. 2, with modified geometry (marked as II_ZB_2_4), were tested. In this case, a symmetrical balcony connection was assumed, with a length of 220 mm, connected at the bottom with two transverse plates with a height of 35 mm and a thickness of 12 mm, located 20 mm from the bottom of the balcony connection. This resulted in the reduction of the effective depth of the cross-section (by lifting of transverse plate up on the ceiling slab) and the elongation of the anchorage length in the ceiling slab.

The variable parameters in the analysis were:
1. use of a muff to connect the longitudinal reinforcement bars in balcony sets: II_ZB_2_2, II_ZB_2_3 and II_ZB_2_4 – see Fig. 4 (no muff in Stage I of tests – described in Solarczyk et al. (2020) – I_ZB_2_4 – see Fig. 3); muffs located on two sides of the balcony connections: approximately 20 cm from the edge of ceiling slab and 25 cm from the edge of balcony slab; total distance between muffs – 51.7 cm;
2. two-stages of concreting – balcony slab build two days earlier than ceiling slab (in balcony set II_ZB_2_2);
3. modified geometry of balcony connection – application of symmetrical balcony connection (to eliminate assembly problems) and elongation of anchorage length in ceiling slab (in balcony set II_ZB_2_4) (Fig. 2).
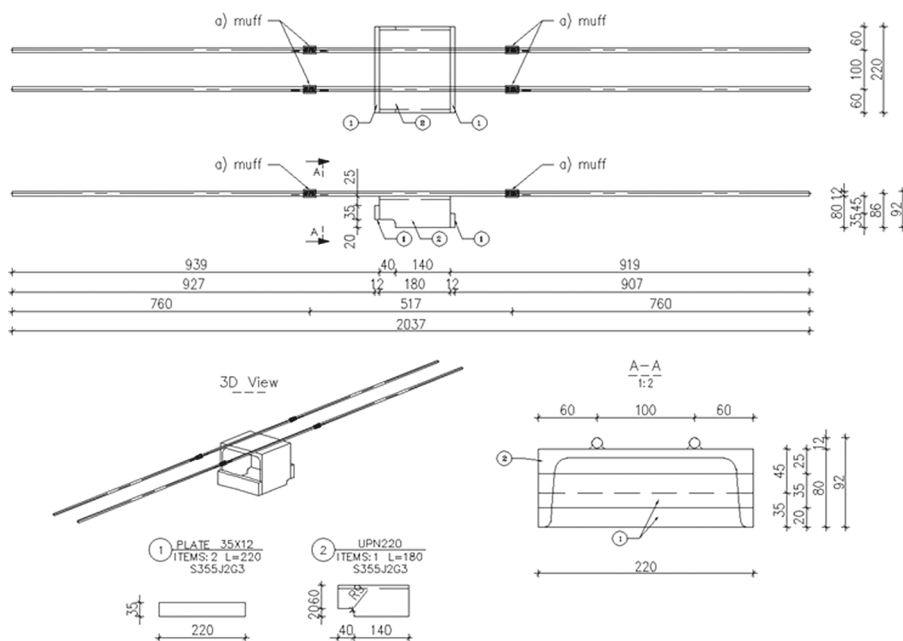

Fig. 1. The geometry of balcony connection: in Stage I (without muff) – set I_ZB_2_1 and in Stage II (with muff): II_ZB_2_2 and II_ZB_2_3 [own study]

In Stage II of the tests, muffs on the longitudinal reinforcement bars were used to simplified the assembly of the balcony connections (see the geometry at Fig. 1 and Fig. 2). Additionally, the balcony connection with a muff to enable corrosion protection by hot-dip galvanizing (with a minimum galvanized coating thickness of 85 μm) was made. The anticorrosive protection in the balcony connection zone between the balcony and the ceiling is intended to protect the element against the possible ingress of water from the top of the balcony into the balcony connection interior, and also to protect the connection against corrosion in the zone of the possible condensation of water vapor.
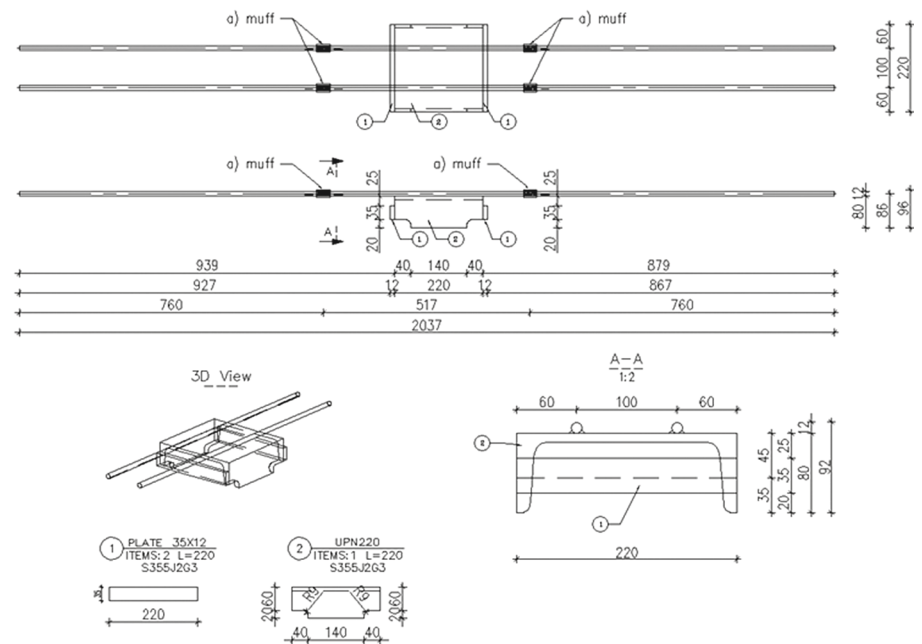

Fig. 2. The geometry of the balcony connection in Stage II (with muff) – set II_ZB_2_4 (the geometry of balcony connection has been modified in relation to Stage I) [own study]

2. Literature

An overview of system solutions for balcony connections was presented in a paper by Solarczyk et al. (2021).

Susorova et al. (2019) presented a numerical and experimental analysis of the temperature distribution at the wall-balcony interface and the impact of the use of thermal connections on the energy consumption in the building over the annual cycle. The research was carried out on eight balconies (four with thermal balcony connections and four control connections without thermal insulation) using the example of a multi-family building in Chicago. Temperature sensors were embedded into eight balconies and their adjacent interior floor slabs just before concreting. The measurements were carried out continuously over a period of one year. The results demonstrate that the thermal breaks in the balcony reduce the linear thermal bridge, but the predicted effect on annual energy consumption in all modelled building types was small (less than 2%).

Pawłowski (2021) presents examples of numerical calculations of balcony joints in terms of their thermal and humidity requirements. Special attention was paid to the necessity to carefully select materials of external walls and the balcony slab in order to ensure appropriate physical parameters of the element.

The thermal aspects of the reinforced concrete balcony – floor connection are presented by Dikarev et al. (2015). The results of thermal imaging tests on the existing building are described, laboratory tests of the balcony-floor connection with and without thermal connectors are presented, and the numerical analysis performed with the use of the ANSYS software is presented.

In terms of structural behaviour, the issue of balcony connections was presented by Heidolf and Eligehausen (2013), in which the authors presented

a design concept of connections with compression shear bearings. The paper describes the results of experimental and numerical investigations of load-bearing capacity and the deformation of balcony connections. In addition, the failure mechanism is discussed and a developed method of designing is described.

Le Bloa et al. (2017) describes a floor to balcony junction made as a thermal connection with a special construction element – stainless steel Z-shaped profile. The authors of the paper draw attention to the complex work of such an element and thus to experimental studies covering different M/V ratios varying from 0.1 to 0.8. An analytical model have been deduced in order to predict the resistance at ULS (Ultimate Limit State) of the balcony connection.

Keo et al. (2018) summarises the experimental tests of balcony connections subjected to vertical actions. An analytical formula to determine the load-bearing capacity of the connection was proposed, as well as a model for calculating bending stiffness, confirmed by the results of experimental tests.

3. Tests of balcony connection

The authors tested four full-scale prefabricated balcony sets with dimensions (width × length × height): 2.0 m × 2.78 m × 0.186 m (in a slope to 0.17 m). The assumed differences between the sets are discussed in point 1 of the paper. The sets consists of reinforced concrete slabs (balcony and ceiling) connected with each other by double-type balcony connections (Fig. 5 and Fig. 6). In each set, six balcony connections were used to connect slabs (one connection – a C-section with two welded reinforcing bars ϕ12 mm), divided into two packages of three connections, 0.66 m length, spaced every 0.10 m within C-section and 0.12 m between the next balcony connection. The overhang of the cantilever (measured to the edge of ceiling slab) equals L_{eff} = 1.78 m. Concrete C30/37 and reinforcement steel K500-B-T were used to build the balcony sets.
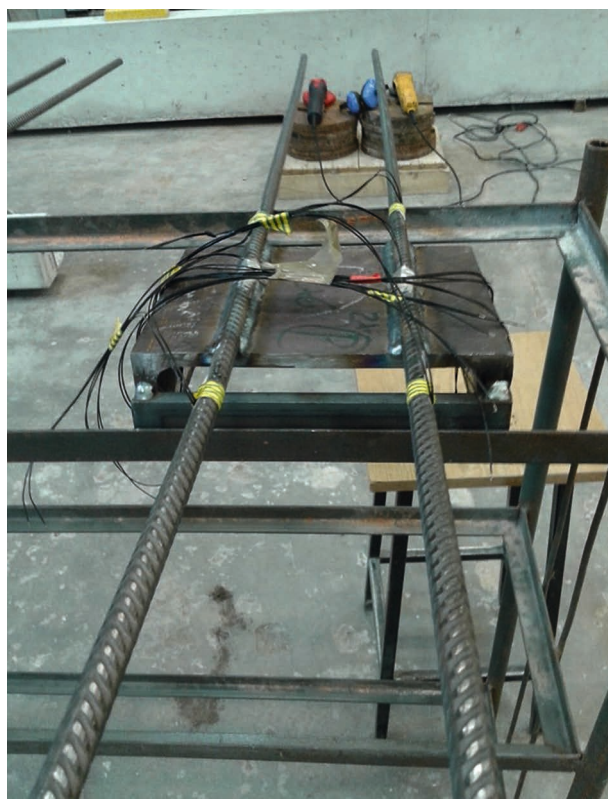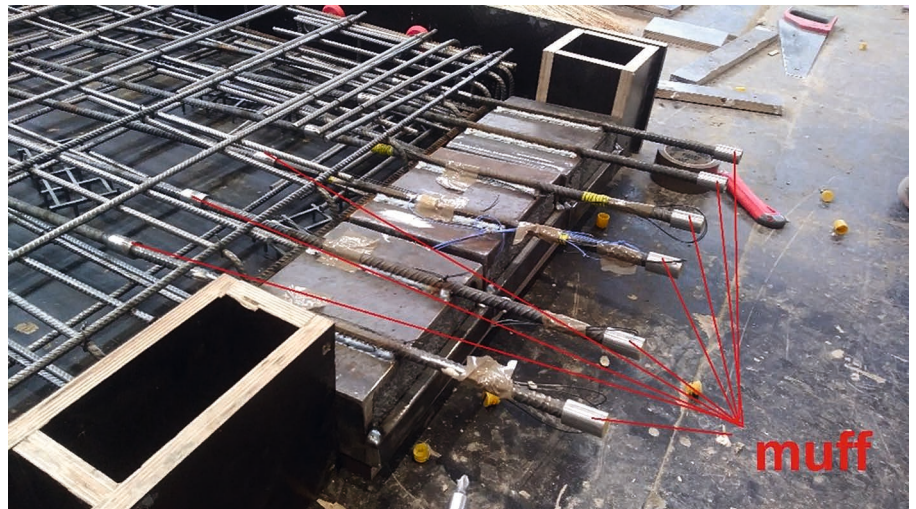

Fig. 3. Balcony connection with glued strain gauges before assembly of reinforcement in set I_ZB_2_1 – without muff on longitudinal reinforcement bars (Stage I) [own study]

Fig. 4. Balcony connection with glued strain gauges before concreting set II_ZB_2_3 – muff on longitudinal reinforcement bars (Stage II) [own study]

The tests were carried out on the test stand described in Solarczyk et al. (2020). It was assumed that balcony sets would be loaded quasi linearly, parallel to the outer edge of balcony slab by use of set of beams on which the concentrated load (F) of the hydraulic jack of the testing machine is applied.

During tests, deflections in three points at the end of cantilever were measured using displacement sensors with an accuracy of 0.01 mm. Additionally, crack morphology with measurement of crack width (by microscope with accuracy of 0.02 mm) and strains of steel (strain gauges with an accuracy of $0.1 \times 1/200$ mm/m) were tested.

In balcony set I_ZB_2_1 a 36 strain gauges (Fig. 5), while in II_ZB_2_2, II_ZB_2_3 and II_ZB_2_4 a 12 strain gauges in each balcony sets were used (Fig. 6).

Strain gauges in strain diagrams of balcony connections were marked as follows:

$$\underset{(1)}{1} \_ \underset{(2)}{T1}$$

where: (1) – (1, 2, 3, 4, 5, 6, 6', 5', 2' or 1') – reinforcement bar on which a strain gauge was glued – numeration according to Fig. 5 and Fig. 6, (2) – (T1, T2, T3, T4, T5 or T6) – number of strain gauge – numeration according to Fig. 5 and Fig. 6.
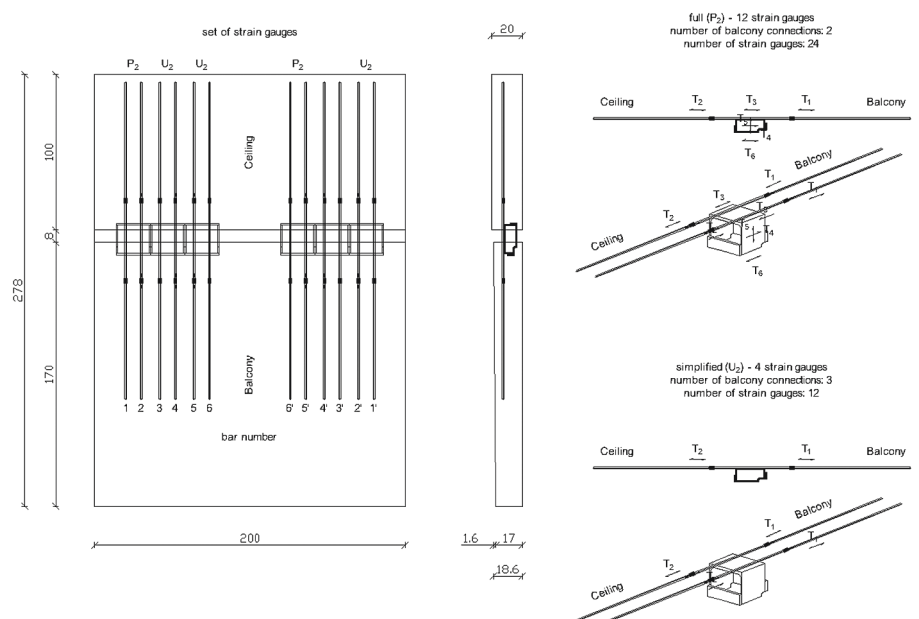

Fig. 5. Arrangement of strain gauges on double-type balcony connection during Stage I of tests [own study]
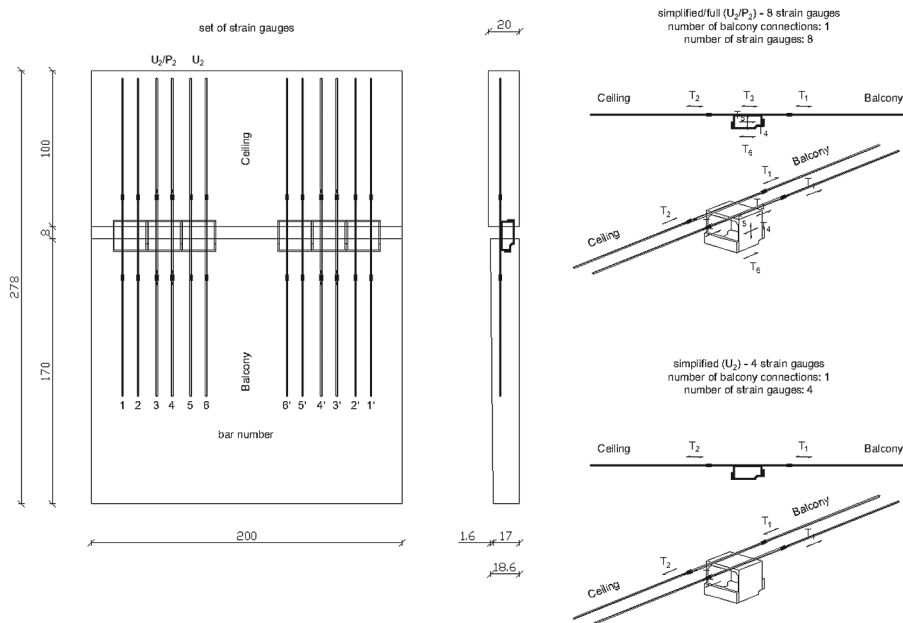
Fig. 6. Arrangement of strain gauges on double-type balcony connection during Stage II of tests [own study]

In terms of strain in steel measurements, the following sign convention was assumed: „+" denotes compression and „−" denotes tension.

In the strain diagrams in section 3.1–3.4 (Fig. 7, Fig. 8, Fig. 9, Fig. 10, Fig. 13 and Fig. 16), example results of tests for each of measured points are shown (from T1 to T6).

The maximum value of load obtained in tests was assumed as the failure force (F_u). During testing, the value of the force was taken as the load from the hydraulic jack of the Zwick – Roell 500 kN testing machine, given with an accuracy of 0.1 kN.

3.1. Balcony set I_ZB_2_1

The deflection diagram and crack morphology in set I_ZB_2_1 were presented in Fig. 10 and Fig. 11 in Solarczyk et al. (2020).

The amount of strains in gauges placed on bars (see T1 and T2 – Fig. 7 and Fig. 8) showed that most of the load was taken by the bars on the ceiling slab (T2). The first bars on the ceiling slab (Fig. 8) reaches the yielding point at a load level (F/F_u) of about 0.5, while on the balcony slab (Fig. 7) this point is reached at a load level of about 0.55 – 0.95.
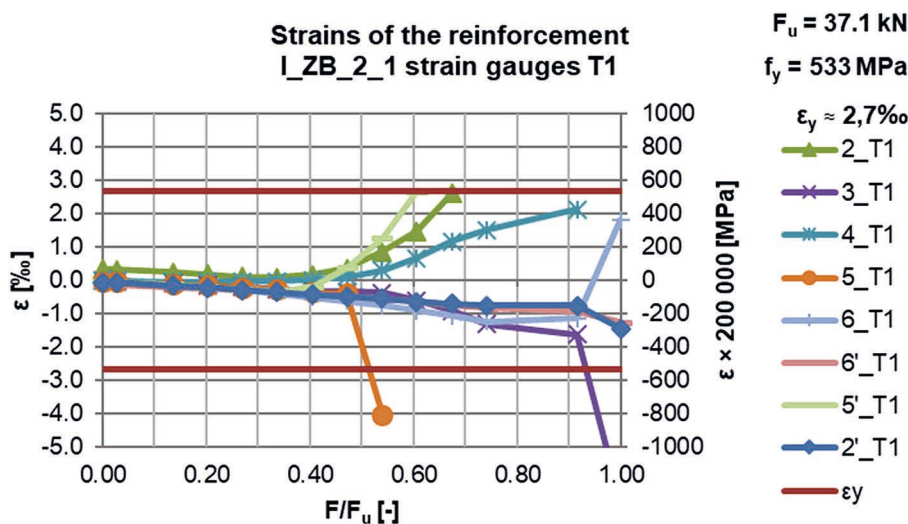

Fig. 7. Strains of the reinforcement in balcony set I_ZB_2_1 measured for T1 strain gauges during Stage I of tests [own study]
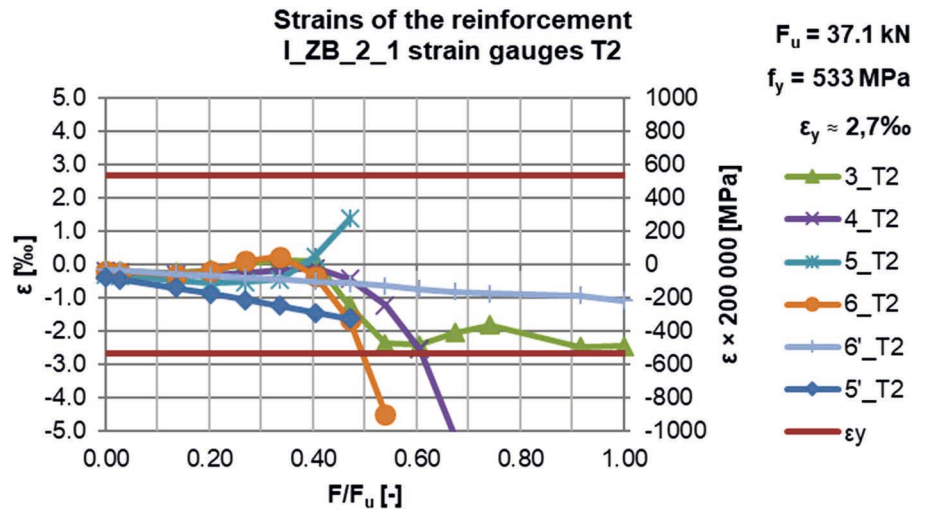
Strains of the reinforcement I_ZB_2_1 strain gauges T2

$F_u = 37.1$ kN
$f_y = 533$ MPa
$\varepsilon_y \approx 2{,}7‰$

Fig. 8. Strains of the reinforcement in balcony set I_ZB_2_1 measured for T2 strain gauges during Stage I of tests [own study]

Strains of the reinforcement I_ZB_2_1 strain gauges T3

$F_u = 37.1$ kN
$f_y = 533$ MPa
$\varepsilon_y \approx 2{,}7‰$
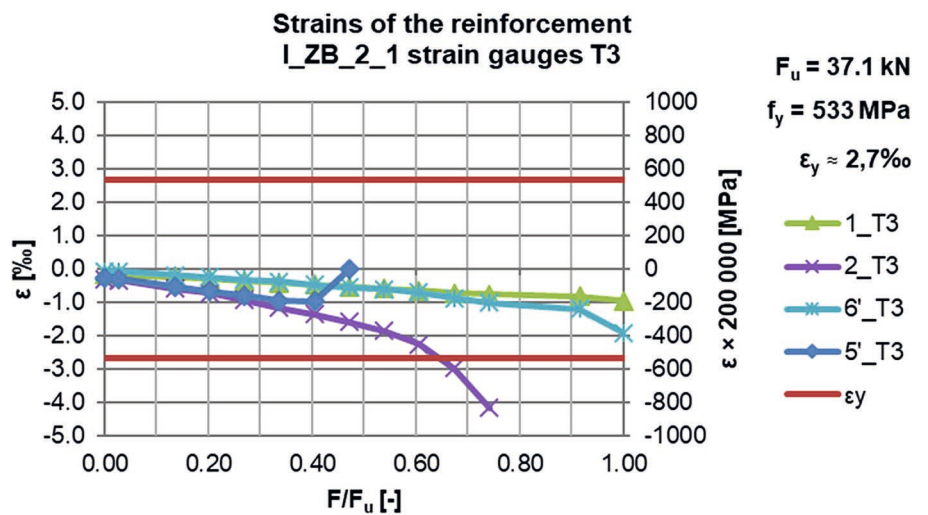
Fig. 9. Strains of the reinforcement in balcony set I_ZB_2_1 measured for T3 strain gauges during Stage I of the tests [own study]

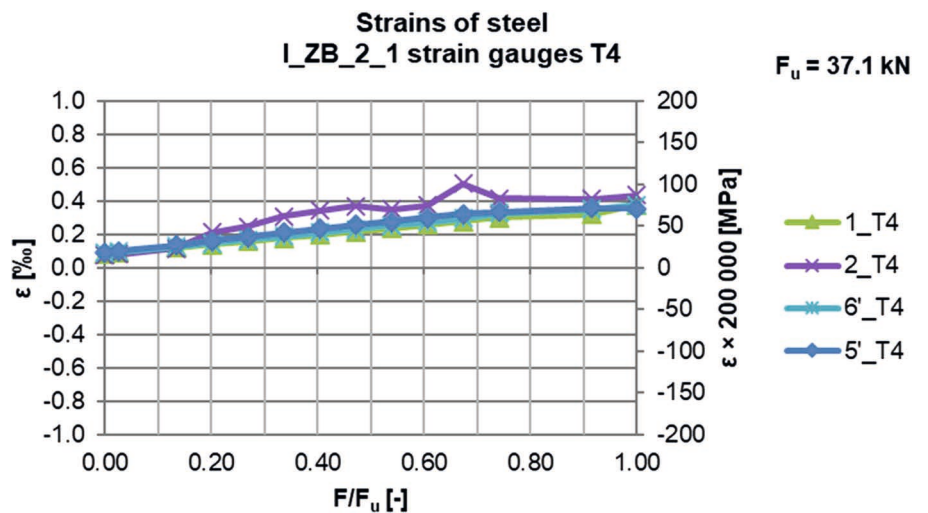**Strains of steel I_ZB_2_1 strain gauges T4**

$F_u = 37.1$ kN

Fig. 10. Strains of steel in balcony set I_ZB_2_1 measured for T4 strain gauges during Stage I of the tests [own study]

Strain gauge T3 (Fig. 9) was placed on the top of the balcony connection (in the middle), on the reinforcement bar welded to the web of the C-profile. The values of stresses in the steel show that the C-profile increases the stiffness of the balcony connection. Tensile stresses values were below the yield point (except 2_T3 strain gauge), and were lower than stresses obtained in the T1 and T2 strain gauges (Fig. 7, Fig. 8 and Fig. 9).

For strain gauge T4 (placed in the middle of flange of C-profile – horizontally; see Fig. 5 and Fig. 6), a gradual increase of compressive stresses were observed, reaching the value of σ = 100 MPa at failure (below the yield point of C-section steel).

3.2. Balcony set II_ZB_2_2

Strain gauge T6 (Fig. 13) was placed on the bottom of the balcony connection, compressive stresses (gradually increasing) were observed, reaching up to σ = 250 MPa at failure (below the yield point of C-section steel).
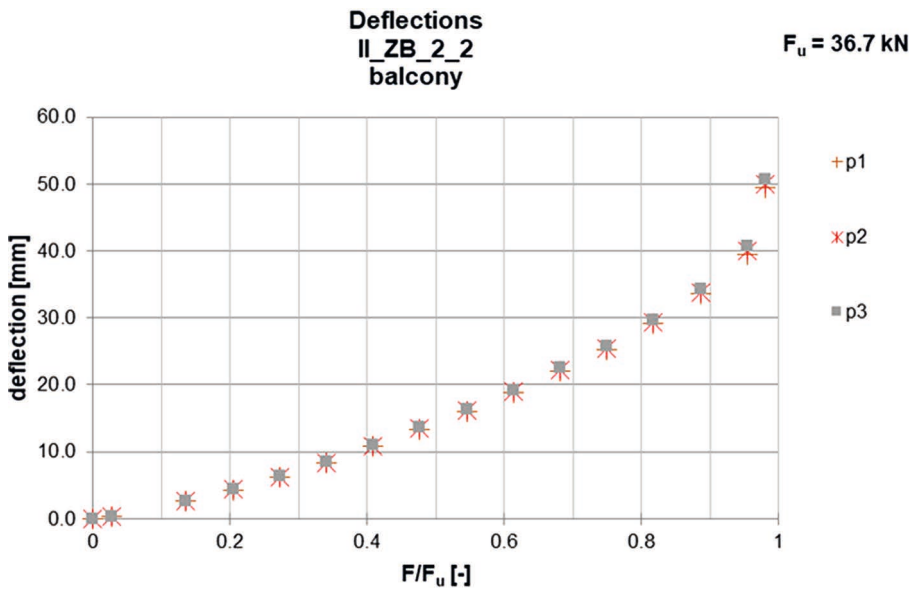

Fig. 11. Deflection of balcony set II_ZB_2_2 during Stage II of tests [own study]

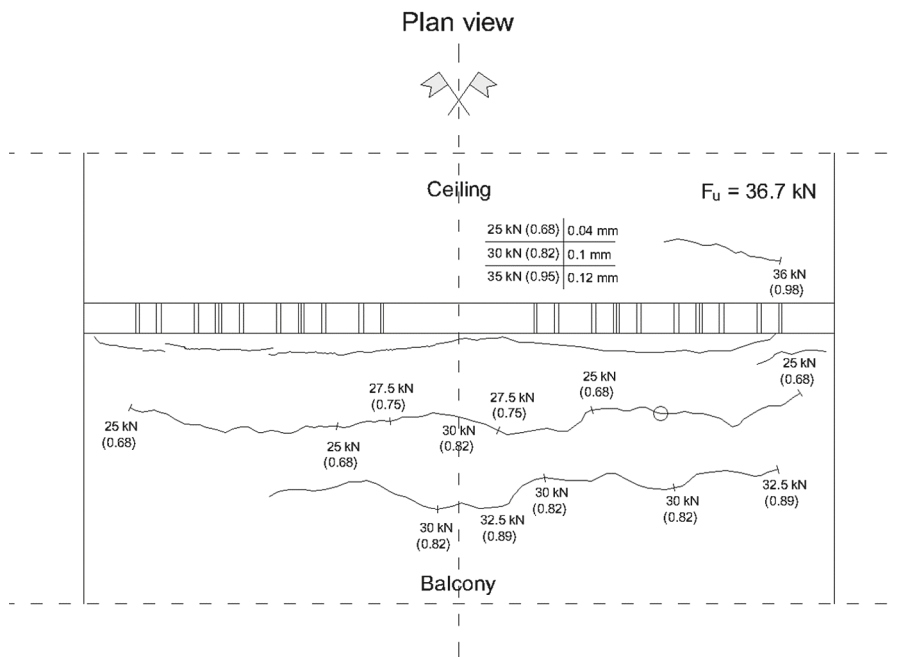**Fig. 12.** Crack morphology of balcony set II_ZB_2_2 during Stage II of tests [own study]

Fig. 13. Strains of steel in balcony set II_ZB_2_2 measured for T6 strain gauges during Stage II of tests [own study]

3.3. Balcony set II_ZB_2_3

Fig. 14. Deflection of balcony set II_ZB_2_3 during Stage II of tests [own study]

Fig. 15. Crack morphology of balcony set II_ZB_2_3 during Stage II of tests [own study]

Strain gauge T5 (placed in the middle of flange of C-profile – vertically; Fig. 5 and Fig. 6) compressive stresses (Fig. 16) were observed, reaching a value of σ = 100 MPa at failure.

Fig. 16. Strains of steel in balcony set II_ZB_2_3 measured for T5 strain gauges during Stage II of tests [own study]

3.4. Balcony set II_ZB_2_4

Fig. 17. Deflection of balcony set II_ZB_2_4 during Stage II of tests [own study]

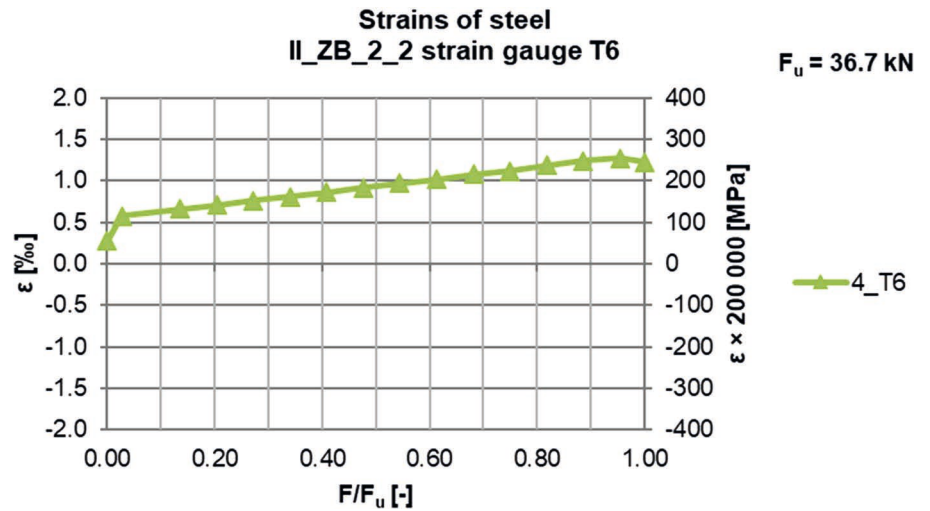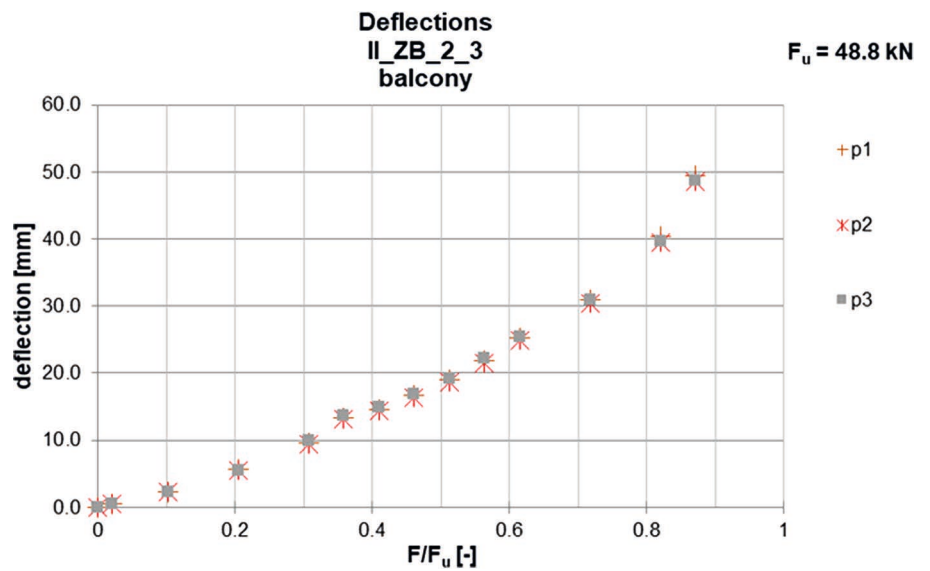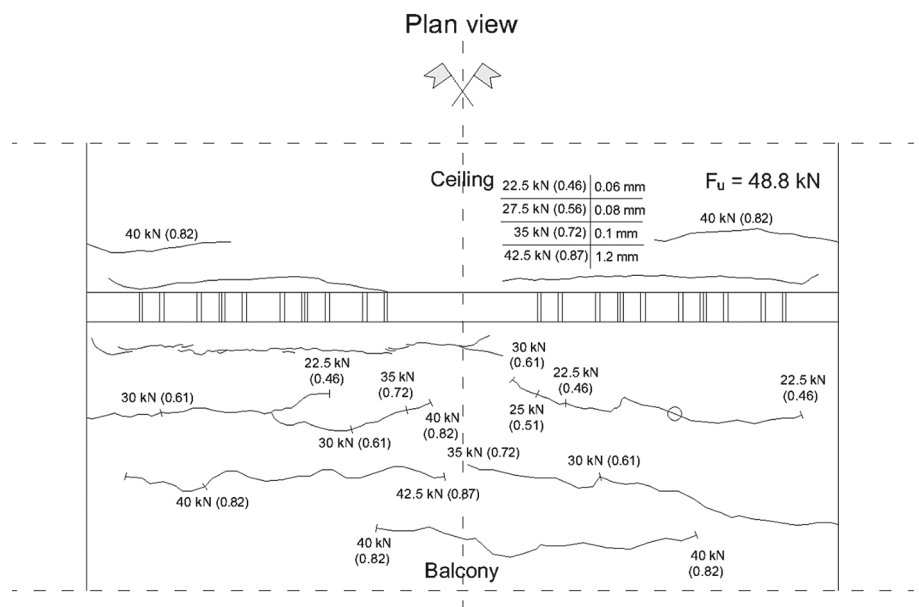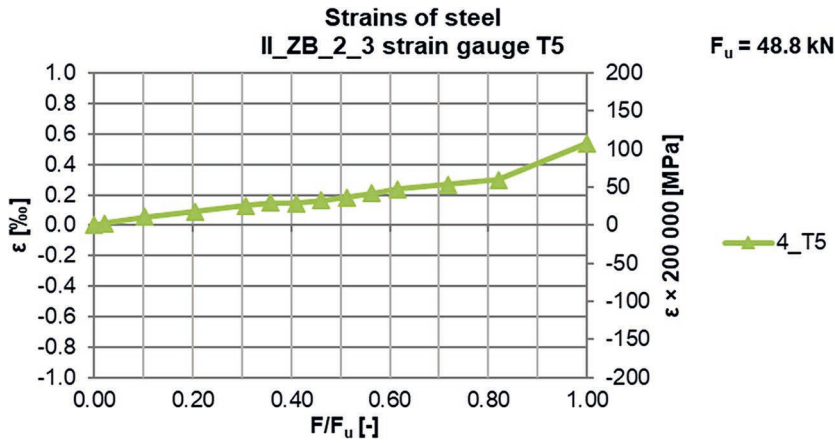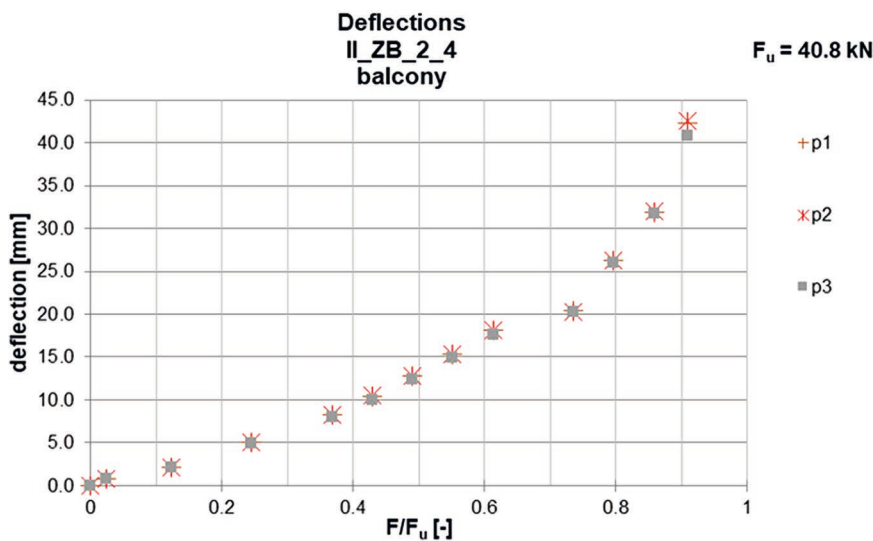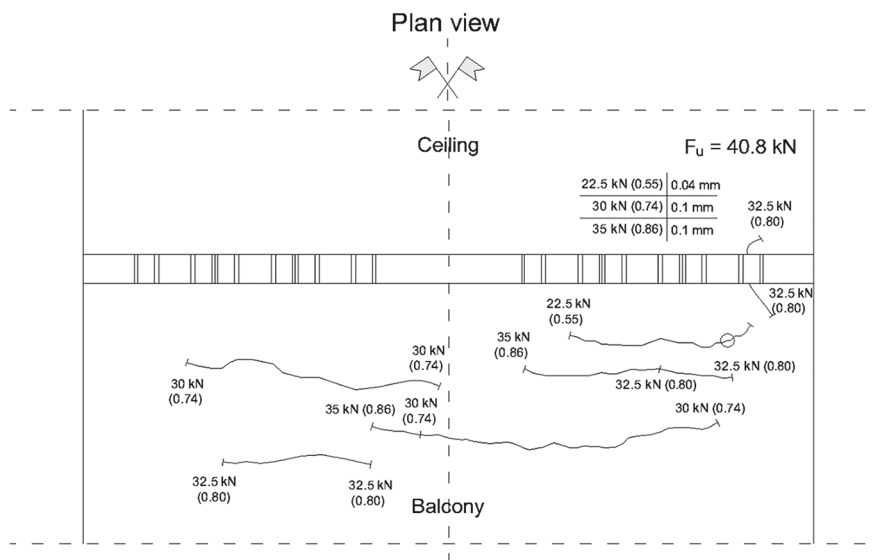**Fig. 18.** Crack morphology of balcony set II_ZB_2_4 during Stage II of tests [own study]

4. Static calculations

Permissible value of deflection (according to 7.4.1 (4) in EN 1992-1-1:2004):

$$f_{\lim} = \frac{1}{250} \cdot L_{\text{eff}} = 0.71 \, \text{cm}$$

According to Table 8 in PN-B–03264: 2002 the limit deflection for cantilever equals:

$$f_{\lim, \text{PN-B}} = \frac{L_{\text{eff}}}{150} = 1.19 \, \text{cm}$$

Total bending moment determined from standard EN 1991–1-1:2002 actions (characteristic value) – calculations was presented in Solarczyk et al. (2020):

$$M_{\text{Ek}} = 39.5 \, \text{kNm}$$

Section modulus before cracking for balcony:

$$W = \frac{B \cdot h^2}{6} = 11532.0 \, \text{cm}^3$$

Characteristic yield strength of reinforcement:

$$f_y = 533 \, \text{MPa}$$

(obtained from testing samples of reinforcing bars with a diameter of $\phi 12$ mm).
Effective depth of cross section:

$$d = 8.6 \, \text{cm}$$

(for II_ZB_2_4: $d = 6.6$ cm – measured from the bottom of the transverse plate of the balcony connection).
As lever arm of internal forces z, the distance between the centroid of the tension reinforcement of the balcony and the centroid concrete compression force (which was calculated as the force acting on the transverse plate of the balcony connection) was assumed.

4.1. Balcony set I_ZB_2_1

Mean value of concrete compressive strength:

$$f_{\text{cm}} = 39.1 \, \text{MPa}$$

Calculated cracking moment:

$$M_{\text{cr, calc}} = W \cdot f_{\text{ctm}} = 34.2 \, \text{kNm}$$

Resistance due to bending moment (characteristic and design value):

$$M_{\text{Rk}} = A_{s1} \cdot f_y \cdot z = 13.57 \, \text{cm}^2 \cdot 53.3 \, \frac{\text{kN}}{\text{cm}^2} \cdot 7.9 \, \text{cm} = 57.1 \, \text{kNm}$$

$$M_{\text{Rd}} = A_{s1} \cdot f_{yd} \cdot z = 13.57 \, \text{cm}^2 \cdot \frac{53.3 \, \frac{\text{kN}}{\text{cm}^2}}{1.15} \cdot 7.9 \, \text{cm} = 49.7 \, \text{kNm}$$

4.2. Balcony set II_ZB_2_2

For ceiling: mean value of concrete compressive strength:

$$f_{cm} = 48.2 \, \text{MPa}$$

For balcony: mean value of concrete compressive strength:

$$f_{cm} = 38.1 \, \text{MPa}$$

Calculated cracking moment:

$$M_{cr,calc} = W \cdot f_{ctm} = 33.4 \, \text{kNm}$$

Resistance due to bending moment (characteristic and design value):

$$M_{Rk} = A_{s1} \cdot f_y \cdot z = 13.57 \, \text{cm}^2 \cdot 53.3 \, \frac{\text{kN}}{\text{cm}^2} \cdot 8.0 \, \text{cm} = 58.1 \, \text{kNm}$$

$$M_{Rd} = A_{s1} \cdot f_{yd} \cdot z = 13.57 \, \text{cm}^2 \cdot \frac{53.3 \, \frac{\text{kN}}{\text{cm}^2}}{1.15} \cdot 8.0 \, \text{cm} = 50.5 \, \text{kNm}$$

4.3. Balcony set II_ZB_2_3

Mean value of concrete compressive strength:

$$f_{cm} = 38.2 \, \text{MPa}$$

Calculated cracking moment:

$$M_{cr,calc} = W \cdot f_{ctm} = 33.4 \, \text{kNm}$$

Resistance due to bending moment (characteristic and design value):

$$M_{Rk} = A_{s1} \cdot f_y \cdot z = 13.57 \, \text{cm}^2 \cdot 53.3 \, \frac{\text{kN}}{\text{cm}^2} \cdot 7.9 \, \text{cm} = 57.0 \, \text{kNm}$$

$$M_{Rd} = A_{s1} \cdot f_{yd} \cdot z = 13.57 \, \text{cm}^2 \cdot \frac{53.3 \, \frac{\text{kN}}{\text{cm}^2}}{1.15} \cdot 7.9 \, \text{cm} = 49.6 \, \text{kNm}$$

4.4. Balcony set II_ZB_2_4

Mean value of concrete compressive strength:

$$f_{cm} = 48.1 \, \text{MPa}$$

Calculated cracking moment:

$$M_{cr,calc} = W \cdot f_{ctm} = 40.4 \, \text{kNm}$$

Resistance due to bending moment (characteristic and design value):

$$M_{Rk} = A_{s1} \cdot f_y \cdot z = 46.4 \, \text{kNm}$$

$$M_{Rd} = A_{s1} \cdot f_{yd} \cdot z = 44.1 \, \text{kNm}$$

5. Analysis of research results

Table 1. Summary of characteristic values obtained from tests and analysis of results for double-type balcony connections in Stages I and II of tests

Description	test / calc	symbol [unit]	I_ZB_2_1	II_ZB_2_2	II_ZB_2_3	II_ZB_2_4
				− muff − two-stage concreting	− muff	− muff − modified geometry of balcony connection
force from the hydraulic jack of testing machine at which an equivalent bending moment due to standard actions was obtained	test	F_{Ek} [kN]	14.2	14.3	14.3	14.6
bending moment determined from standard actions (load level)	calc	M_{Ek} [kNm]	39.5 (0.53)	39.5 (0.54)	39.5 (0.43)	39.5 (0.50)
deflection at force F_{Ek}	test	f_{Ek} [mm]	11.3	11.0	9.9	8.3
cracking force	test	F_{cr} [kN]	30.0	25	22.5	22.5
maximum measured deflection before failure (load level)	test	$f_{max,test}$ [mm]	39.8 (0.92)	50.8 (0.98)	49.5 (0.87)	42.6 (0.91)
maximum measured crack width before failure	test	[mm]	0.1	0.12	1.2	0.1
resistance due to bending moment	calc	M_{Rk} [kNm]	57.1	58.1	57.0	46.4
failure force	test	F_u [kN]	**37.1**	**36.7**	**48.8**	**40.8**
failure moment	test	M_u [kNm]	**74.4**	**73.4**	**91.7**	**78.6**
mode of the failure	test		*pull out of balcony connections from ceiling slab*	*pull out of balcony connections from ceiling slab*	*pull out of balcony connections from ceiling slab*	*pull out of balcony connections from ceiling slab*

Maximum crack width measured before failure equals w_{max} = 1.2 mm (see Fig. 15 – set II_ZB_2_3). In other cases, crack width does not exceed the standard limiting value EN 1992-1-1:2004 and PN-B 03264:2002: w_{lim} = 0.3 mm.

The failure of all tested balcony sets was caused by gradual pulling out of the balcony connections from the concrete of the ceiling slab. At that time, cracks and fragments of concrete which had split off from the front of ceiling slab were visible. This corresponded to a significant deflection of about 19 cm.

Table 2. Summary of the determined safety factors and load-level factors for double-type balcony connections in Stages I and II of tests

Description	symbol		I_ZB_2_1	II_ZB_2_2	II_ZB_2_3	II_ZB_2_4
ratio of the calculated resistance to failure moment	calc / test	$\eta_u = \dfrac{M_{Rk}}{M_u}$	0.77	0.79	0.62	0.59
load level from standard actions	calc / test	$\eta_u = \dfrac{M_{Ek}}{M_u}$	0.53	0.54	0.43	0.50
global safety factor	test / calc	$\gamma = \dfrac{M_u}{M_{Ek}}$	**1.88**	**1.86**	**2.32**	**1.99**

Under the applied standard EN 1991–1-1:2002 actions (see force F_{Ek}) the maximum measured deflection (I_ZB_2_1) was f = 11.3 mm and was lower

than the permissible value of deflection limited to 1/150 of cantilever. Due to the creep coefficient in quasi-permanent combination of actions, it may happen that the permissible deflection of the element will determine the quantity or type of used balcony connections or the execution of the upward deflection of the balcony.

6. Conclusions

The mode of the failure of all tested sets was similar and showed gradually pull out of balcony connections from the ceiling slab and fragments of concrete that had split off from the front of the ceiling slab were visible. The pull out of balcony connections occurred in subsequent steps of loading after reaching the failure force, in which the deflection increased (rotation of the balcony connection), with the decrease in force.

Deflections measured before reaching the maximum force – before failure (at the load level $\eta = 0.9$) did not exceed $f = 50$ mm.

Calculated resistance due to bending moment M_{Rk} (assuming yielding in reinforcement bars of balcony connections) related to failure moment M_u was on average $\eta_u = \dfrac{M_{Rk}}{M_u} = 0.69$.

For balcony connections, the average global safety factor was $\gamma = 2.01$, while in three out of four sets, the global safety factor was lower than 2.0.

Despite the increase in anchorage length of the balcony connection in the ceiling slab (set II_ZB_2_4), no significant increase of load-bearing capacity was observed. The reduction of effective depth of a cross section is the reason for this and it is not compensated by the increase of anchorage length.

Modified geometry of balcony connection (elongation of anchorage) in set II_ZB_2_4 reduced the deflection of the balcony (see Fig. 19). Under standard EN 1991–1-1:2002 actions, balcony connection II_ZB_2_4 obtained the lowest deflection of all tested sets, which was 8.3 mm.
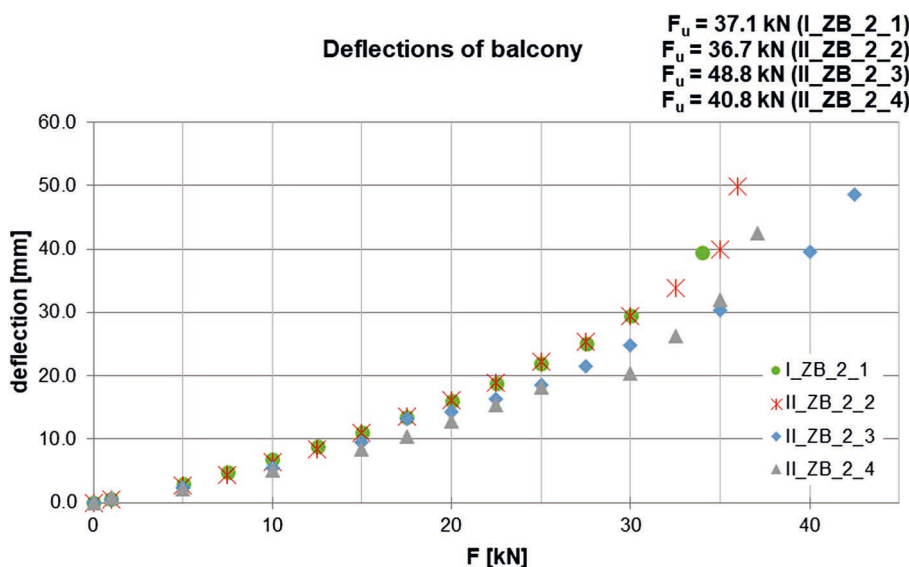

Fig. 19. Comparison of deflections of balcony sets during Stages I and II of tests [own study]

No negative effects on use of muff on longitudinal reinforcement bars were observed.

Concreting the elements in two stages (ceiling slab and balcony slab build with a two-day interval) did not result in significant changes in the load-bearing capacity of the balcony sets.

References

Dikarev, K., Berezyuk, A., Kuzmenko, O., Skokova, A. (2015). Experimental and numerical thermal analysis of joint connection «floor slab – balcony slabe» with integrated thermal break. *Sustainable Solutions for Energy and Environment, EENVIRO – YRC 2015*, 184–192. http://doi.org/10.1016/j.egypro.2015.12.325

EN 1991–1-1:2002; Eurocode 1: Actions on structures – Part 1-1: General actions – Densities, self-weight, imposed loads for buildings.

EN 1992-1-1:2004; Eurocode 2: Design of concrete structures – Part 1-1: General rules and rules for buildings.

Heidolf, T., Eligehausen, R. (2013). Bemessungskonzept für wärmedämmende Plattenanschlüsse mit Druckschublagern. *Beton- und Stahlbetonbau*, 108(3), 179–187. http://doi.org/1010.1002/best.201200073

Keo, P., Le Gac, B., Somja, H., Palas, F. (2018). Experimental study of the behavior of a steel-concrete hybrid thermal break system under vertical actions. In: *High Tech Concrete: Where Technology and Engineering Meet* (pp. 2573–2580). http://doi.org/1010.1007/978-3-319-59471-2_293

Le Bloa, G., Somja, H., Palas, F. (2017). Experimental Study on the M-V Interaction of a Hybrid Steel Connection Used in Concrete Floor--to-Balcony Junction. In: *High Tech Concrete: Where Technology and Engineering Meet* (pp. 2407–2414). http://doi.org/1010.1007/978-3-319-59471-2_274

Pawłowski, K. (2020). Balkony – projektowanie numeryczne złączy z uwzględnieniem wymagań cieplno-wilgotnościowych od 1 stycznia 2021 roku. *Izolacje*, 4, 28–35.

PN-B 03264:2002: Konstrukcje betonowe, żelbetowe i sprężone – Obliczenia statyczne i projektowanie.

Solarczyk, M. T., Piotrkowski, P., Niedostatkiewicz, M. (2019). Wstępne badania eksperymentalne stalowych łączników balkonowych w aspekcie nośności złącza balkon – strop. In: W. Drozd, K. Zima, P. Kozioł, M. Kowalik (Eds.), 65. *Konferencja Naukowa Komitetu Inżynierii Lądowej i Wodnej PAN oraz Komitetu Nauki PZITB. Krynica 2019, Krynica Zdrój, 15–20.09.2019 r. Materiały konferencyjne*. Kraków: Politechnika Krakowska.

Solarczyk, M. T., Piotrkowski, P., Niedostatkiewicz, M. (2020). Wstępne badania eksperymentalne stalowych łączników balkonowych w aspekcie nośności złącza balkon – strop. In W. Drozd, P. Kozioł, K. Zima (Eds.), Wybrane problemy naukowe budownictwa 65. *Konferencja Naukowa Komitetu Inżynierii Lądowej i Wodnej PAN oraz Komitetu Nauki PZITB* (pp. 13–29). Warszawa: Wydawnictwo Naukowe PWN.

Solarczyk, M. T., Piotrkowski, P., Niedostatkiewicz, M. (2021). Przegląd rozwiązań systemowych łączników balkonowych. *Przegląd Budowlany* 9, 15–23.

Susorova, I., Stephens, B., Skelton, B. (2019). The Effect of Balcony Thermal Breaks on Building Thermal and Energy Performance: Field Experiments and Energy Simulations in Chicago, IL. *Buildings* 9(9):190, 1–24. http://doi.org/10.3390/buildings9090190